

DEUTSCHES ELEKTRONEN-SYNCHROTRON **DESY**

DESY 87-020
March 1987



A NUMERICAL ESTIMATE OF THE UPPER LIMIT FOR THE HIGGS

BOSON MASS

by

W. Langguth

Institut für Theoretische Kernphysik der Universität Karlsruhe

I. Montvay

Deutsches Elektronen-Synchrotron DESY, Hamburg

ISSN 0418-9833

NOTKESTRASSE 85 · 2 HAMBURG 52

DESY behält sich alle Rechte für den Fall der Schutzrechtserteilung und für die wirtschaftliche Verwertung der in diesem Bericht enthaltenen Informationen vor.

DESY reserves all rights for commercial use of information included in this report, especially in case of filing application for or grant of patents.

To be sure that your preprints are promptly included in the
HIGH ENERGY PHYSICS INDEX,
send them to the following address (if possible by air mail) :

**DESY
Bibliothek
Notkestrasse 85
2 Hamburg 52
Germany**

A numerical estimate of the upper limit for the Higgs boson mass

W. Langguth

Institut für Theoretische Kernphysik der Universität Karlsruhe

I. Montvay

Deutsches Elektronen-Synchrotron DESY, Hamburg

March 17, 1987

Abstract

The SU(2) Higgs model with a scalar doublet field is studied by Monte Carlo calculations on 12^4 and 16^4 lattices. The gauge coupling is chosen to be similar in magnitude to the physical value in the standard model. The numerical results at large scalar self-coupling imply an upper limit $m_H/m_W \simeq 9$ for the ratio of the Higgs boson mass to the W-mass.

1 Introduction

Some time ago Dashen and Neuberger [1] suggested to determine the non-perturbative upper limit for the Higgs boson mass within the Higgs sector of the standard model by Monte Carlo calculations. One way to obtain this upper limit is to perform the numerical calculation in the broken symmetry phase of the four-component pure scalar theory and use perturbation theory in order to incorporate the effect of the weak SU(2) gauge coupling. The difficulty one has to face in this way is the presence of infrared singularities due to the zero mass Goldstone bosons. Another possibility is to introduce the weakly coupled gauge field in the Monte Carlo calculation which acts, via the Higgs mechanism, as an infrared regulator. As it was shown recently [2], numerical Monte Carlo calculations are possible also in the physically interesting range of the SU(2) gauge coupling.

The reason for the existence of an upper limit for the Higgs mass is that, as it was assumed also in Ref. [1], the standard Higgs sector is most likely an effective field theory with a necessarily finite cut-off (its continuum limit is trivial [3]). The qualitative behaviour of the renormalization group trajectories (or "curves of constant physics") can be determined for small gauge couplings from the weak gauge coupling expansion (WGCE) [4] around the critical line of the scalar ϕ^4 model. The result is [5] that the curves of constant physics go, for increasing cut-off, in the direction of increasing bare scalar self couplings (λ). Every such curve has an endpoint in the $\lambda = \infty$ plane for some finite cut-off. In other words, the points with maximal cut-off, where "new physics" has to come, are to be found in the $\lambda = \infty$ plane. In addition, WGCE also tells that the ratio $R_{HW} \equiv m_H/m_W$ is a monotonously decreasing

function of the maximal cut-off. Therefore, in those points of the $\lambda = \infty$ plane where the Higgs mass in lattice units is of the order 1 (i. e. the cut-off is of the same order as the Higgs mass), one can obtain an absolute upper limit for the ratio of the Higgs mass to W-mass.

In the present paper we report on a detailed exploratory study of the standard Higgs model in the weak gauge coupling region. The main emphasis is on the investigation of the qualitative behaviour of some physical observables as a function of the bare coupling parameters for weak gauge coupling and large scalar self-coupling. The comparison of the results on 12^4 and 16^4 lattices gives also a first insight into the finite lattice size dependence. For the upper limit of the ratio $R_{HW} = m_H/m_W$ we can only obtain a first crude estimate. A more precise determination of its value has to await future Monte Carlo calculations. The present work is a straightforward continuation of the numerical calculation in Ref. [2] at $(\lambda = 1, \beta = 8)$. In fact, we shall include the 12^4 point obtained there also in the present analysis. In the next Section the numerical results on the Wilson-loop expectation values will be given and the value of the renormalized gauge coupling will be determined from the Yukawa potential between external SU(2) charges. In Section 3 the correlation functions in the Higgs- and W-channels will be summarized and the difficulties of the extraction of the corresponding masses will be discussed. The last Section contains a short summary and the conclusions.

2 The renormalized gauge coupling

The notations used in this paper are identical to those of Ref. [2]. We only repeat here the definition of the lattice action for convenience of the reader. At finite λ we have

$$S_{\lambda,\beta,\kappa} = \beta \sum_P \left(1 - \frac{1}{2} \text{Tr} U_P \right) + \sum_x \left\{ \rho_x^2 - 3 \log \rho_x + \lambda (\rho_x^2 - 1)^2 - \kappa \sum_{\mu>0} \rho_{x+\hat{\mu}} \rho_x \text{Tr} \left(\alpha_{x+\hat{\mu}}^+ U(x, \mu) \alpha_x \right) \right\} \quad (1)$$

In the limit of infinitely strong bare scalar self-coupling ($\lambda = \infty$) the length of the Higgs scalar field is frozen to $\rho_x = 1$ and only the angular Higgs variable $\alpha_x \in SU(2)$ remains:

$$S_{\lambda=\infty,\beta,\kappa} = \beta \sum_P \left(1 - \frac{1}{2} \text{Tr} U_P \right) - \kappa \sum_{x,\mu>0} \text{Tr} \left(\alpha_{x+\hat{\mu}}^+ U(x, \mu) \alpha_x \right) \quad (2)$$

The static energy $V(aR)$ of an external SU(2) charge pair (the "potential") is obtained at lattice distance R from the expectation value of rectangular Wilson-loops $W_{R,T}$, as usual:

$$aV(aR) = - \lim_{T \rightarrow \infty} \frac{1}{T} \log \langle W_{R,T} \rangle \quad (3)$$

The potential is distorted on the lattice by scale breaking lattice artifacts and by finite size effects. In our case, due to the weakness of the SU(2) gauge coupling, these can be corrected for, to a large extent, by comparing the numerical results directly to the lattice potential obtained from a single W-exchange in lattice perturbation theory. The necessary formulas were given in [2]: the renormalized SU(2) gauge coupling $\alpha_{SU(2)}$ at lattice distance R can be obtained from

$$\alpha_{SU(2)}(R) \equiv \frac{a[V(aR) - V(aR - a)]}{3\pi[J(\mu, R - 1, L) - J(\mu, R, L)]} \quad (4)$$

Here $J(\mu, R, L)$ is given on an L^3 lattice by

$$J(\mu, R, L) = \frac{1}{L^3} \sum_{\mathbf{p} \neq \mathbf{0}} \frac{e^{i\mathbf{p}_3 R}}{\mu^2 + \sum_i 4 \sin^2 \frac{p_i}{2}} \quad (5)$$

The numerical value of $J(\mu, R-1, L) - J(\mu, R, L)$ can be easily calculated. In Ref. [2] a few representative examples were given. Unfortunately, there is a small mistake in Table 4 of [2]: the mass in columns 2 and 3 should be read $\mu = 0.20$ instead of $\mu = 0.19$. The expressions in Eqs. (4-5) do not take into account the finite time (T) extension of the lattice: it is assumed that in Eq. (3) the limiting value for $T \rightarrow \infty$ can be obtained numerically to a good approximation. (This point will be discussed below.)

The numerical Monte Carlo calculations were performed partly on the CYBER 205 at the Karlsruhe University and partly on the Fujitsu VP-200 at IABG, Ottobrunn. The updating was done by the Metropolis method with 6 hits per variable (including the Higgs variables α_x, ρ_x as well as the SU(2) link-variable $U(x, \mu)$). The effect of the bare self-coupling λ on the physical observables was investigated for approximately constant expectation value of the gauge invariant link variable L (keeping at the same time the bare gauge coupling β fixed). The definition of L is, together with some other average quantities:

$$L = \left\langle \frac{1}{2} \text{Tr} (\alpha_{x+\hat{\mu}}^+ U(x, \mu) \alpha_x) \right\rangle$$

$$P = \left\langle 1 - \frac{1}{2} \text{Tr} U_P \right\rangle \quad \rho = \langle \rho_x \rangle \quad (6)$$

It is known from previous Monte Carlo studies [6] that keeping L constant for fixed β minimizes the effect of changing λ . (Actually it would be possible to tune the value of L to a better precision than we did, but we did not want to have grotesque hopping parameter values with many digits.) At $\lambda = \infty$ and $\beta = 8$ we have chosen 3 points to look for the dependence on the hopping parameter (κ). The point at $\kappa = 0.42$ was repeated also at $\beta = 10$, in order to have an idea about the dependence on the bare gauge coupling ($\beta \equiv 4/g^2$). The number of Monte Carlo sweeps was between 60000 and 200000 per point. The correlations were measured after every sweep. On the 16^4 lattice the Wilson-loops were calculated only after every 20'th sweep. On the 12^4 lattice separate runs were done, due to some technical reasons, for the correlations and for the Wilson-loops (roughly $\frac{1}{3}$ to $\frac{1}{4}$ of the sweeps was devoted to the Wilson-loops). An estimate of the statistical errors was obtained by binning the data sequences into bins of length 2^k , ($k = 0, 1, 2, \dots$) and estimating the standard deviations from the fluctuations of bin averages. For a summary of the measured points see Table I, where also the values of the average quantities in Eq. (6) are included. The number of points in the 3-dimensional parameter space is not too large, but smaller lattices or less statistics per point would not be appropriate for the questions we are interested in.

A convenient definition of the renormalized gauge coupling in the Monte Carlo calculations is based on the static potential between external charges. In order to obtain the potential, one has to determine the expectation value of Wilson-loops. Our results for the 16^4 points are collected in Table IIIA-D, together with the Creutz-ratios

$$\chi_{R,T} \equiv -\log \frac{\langle W_{R,T} \rangle \langle W_{R-1,T-1} \rangle}{\langle W_{R-1,T} \rangle \langle W_{R,T-1} \rangle} \quad (7)$$

The results on the 12^4 lattice look similar but the errors are about a factor of 3 larger. As an example, the point at $(\lambda = \infty, \beta = 8, \kappa = 0.37)$ is shown in Table IV. For the other 12^4 points see Ref. [7].

The physical quantities of interest, like the potential or the "force" (=potential difference) are functions of several Wilson-loops. In order to obtain an estimate of the statistical error of such quantities, one possibility is to calculate them in data bins and estimate the standard deviations from the fluctuations. The errors of the Creutz-ratios in Table IIIA-D were determined in this way. Another way of estimating the errors is to measure the correlation matrix of the Wilson-loops

$$C_{R_1 T_1, R_2 T_2}^{(W)} \equiv \langle W_{R_1 T_1} W_{R_2 T_2} \rangle - \langle W_{R_1 T_1} \rangle \langle W_{R_2 T_2} \rangle \quad (8)$$

If these numbers are available to a reasonable precision, one can estimate the error of any gentle function of an arbitrary subset $W_{R_1 T_1}, \dots, W_{R_k T_k}$ of the Wilson-loops by assuming a correlated multi-dimensional Gaussian distribution for $W_{R_1 T_1}, \dots, W_{R_k T_k}$. The simplest procedure is to diagonalize the correlation matrix $C^{(W)}$ and produce a random sequence of $W_{R_1 T_1}, \dots, W_{R_k T_k}$ values by Gaussians in the direction of the eigenvectors. An arbitrary function of the Wilson-loops can be calculated on the sequence and the standard deviation gives the desired error estimate. In this way the higher order correlations among $W_{R_1 T_1}, \dots, W_{R_k T_k}$ are neglected, but these are usually unimportant for an error estimate. In fact, applying this method to the Creutz-ratios in Table IIIA-D, the statistical errors can be recovered almost exactly. The correlation matrix $C^{(W)}$ could be determined in our 16^4 runs to a good precision. As an example, a representative sample of the Wilson-loop correlations is included in Table V. (For similar other tables see Ref. [7].) The diagonalization of submatrices of $C^{(W)}$ shows that the largest eigenvalue is usually a factor 20-100 larger than the next one. This implies that the Gaussian fluctuations are almost an order of magnitude larger in the direction of the largest eigenvalue than in other directions. It is not a surprise that the largest eigenvalue belongs to an eigenvector with roughly equal positive components in the direction of every Wilson-loop, whereas the small eigenvalues have eigenvectors with opposite sign components. In other words, the Wilson loops fluctuate mainly coherently. The relative fluctuations are much smaller.

This way of estimating the statistical errors is particularly convenient if, for instance, the question of the errors of some fit parameters arises. (The parameters of a fit can also be considered as functions of the input data.) The error estimate by binning the data sequence and performing the fit in the bins is, of course, possible also in this case, but the recording of all measured data during long runs is usually cumbersome. It costs less effort to measure and collect during the run only the correlation matrix and to do the fits at the end on sequences which are distributed according to the measured Gaussian correlations. (For a more detailed description of this method and for an application to the two-point correlation functions see Ref. [8].)

The errors of the Wilson-loop expectation values are quite small, therefore a relatively precise determination of the Yukawa potential parameters is possible. The main difficulty is, however, to extrapolate in Eq. (3) to $T = \infty$. The simplest method of obtaining aV is to form ratios of two Wilson-loops with a given R and neighbouring T . The best estimate can be obtained from the maximum possible T -value (in our case $T_{max} = 6$ or 8):

$$aV(aR) \simeq \log \frac{W_{R, T_{max}-1}}{W_{R, T_{max}}} \quad (9)$$

Taking this approximation for the potential difference in Eq. (4) gives the Creutz-ratio $\chi_{R,T_{max}}$. The inspection of the logarithmic slopes or Creutz-ratios for increasing T shows, however, that Eq. (9) gives only an upper limit both for the potential and the potential difference, because for fixed R the subsequent values in T are still decreasing. A better extrapolation to $T = \infty$ can be obtained from two-exponential fits of the T -dependence by taking the lower exponent as the $T = \infty$ value. We tried fits in several T -intervals and performed consistency checks. On the 16^4 lattice a good T -extrapolation of the potential could be achieved in this way for $1 \leq T \leq 4$. Apart from a slight, barely significant, increase in the point $(\lambda, \beta, \kappa) = (\infty, 8, 0.34)$, on the 16^4 lattice the renormalized SU(2) coupling $\alpha_{SU(2)}$ obtained from Eq. (4) turned out to be independent of the distance for $2 \leq R \leq 4$:

$$\begin{aligned}
(\infty, 8, 0.34) : \quad \alpha_{SU(2)} &= 0.049 \pm 0.001 \\
(\infty, 8, 0.37) : \quad \alpha_{SU(2)} &= 0.047 \pm 0.001 \\
(\infty, 8, 0.42) : \quad \alpha_{SU(2)} &= 0.048 \pm 0.001 \\
(\infty, 10, 0.42) : \quad \alpha_{SU(2)} &= 0.037 \pm 0.001
\end{aligned} \tag{10}$$

We consider the observed independence on R as a sign of the correctness of T -extrapolation. The difference between the simplest estimate in Eq.(9) and the result of the two-exponential fits is illustrated by Figs. 1A-1D. On the 12^4 lattice the situation is still somewhat more difficult. In the points where both 12^4 and 16^4 were measured, the $\alpha_{SU(2)}$ -values turned out to be about 5% higher on 12^4 . Besides, on the 12^4 lattice there was still some increase also for $2 \leq R \leq 4$. As a summary, we quote for $2 \leq R \leq 4$:

$$\begin{aligned}
(0.1, 8, 0.177) : \quad \alpha_{SU(2)} &= 0.049 \pm 0.001 \\
(1.0, 8, 0.28) : \quad \alpha_{SU(2)} &= 0.050 \pm 0.001 \\
(\infty, 8, 0.37) : \quad \alpha_{SU(2)} &= 0.051 \pm 0.002 \\
(\infty, 8, 0.42) : \quad \alpha_{SU(2)} &= 0.051 \pm 0.002
\end{aligned} \tag{11}$$

A precise definition of the renormalized gauge coupling has to specify the value of the distance R , too, where $\alpha_{SU(2)}(R)$ is taken. A possible choice is, for instance, $R \simeq (am_W)^{-1}$ which means in our case (as we shall see below) $R \simeq 4 - 7$. Unfortunately, the time extension of our 16^4 lattice does not allow for a reliable determination of $\alpha_{SU(2)}$ for $R > 4$. On a somewhat formal level we can take in the definition of the renormalized gauge coupling, for instance, $R \simeq (2am_W)^{-1}$ and use the values in Eq. (10). Of course, in future Monte Carlo studies it would be interesting to check the R -dependence of $\alpha_{SU(2)}$ also in the range of $R \sim (am_W)^{-1}$.

The renormalized SU(2) coupling is usually defined by the W-exchange between fermions and not by the Yukawa potential. Since in our case the lattice scale is of the order of m_W , the best we can do is to compare to the usual coupling at the scale m_W . Taking $\alpha_{em}(m_W) = (128)^{-1}$ [9] and $\sin^2 \theta_W(m_W) = 0.226$ [10] one has for the usual renormalized SU(2) coupling:

$$\alpha_2(m_W) \simeq 0.035 \tag{12}$$

Among the values in Eq. (10) the last one, in the point $(\lambda, \beta, \kappa) = (\infty, 10, 0.42)$, is closest to this.

3 The mass of the W-boson and Higgs boson

The masses were determined from the same two-point correlations as in Ref. [2]. For $\lambda < \infty$ we considered in the W-channel, with $V(x, \mu) \equiv \alpha_{x+\hat{\mu}}^+ U(x, \mu) \alpha_x$:

$$w_{x\tau\mu} = \begin{cases} w_{x\tau\mu}^{(1)} \equiv \text{Tr}(\tau_r V(x, \mu)) & (\tau = 1, 2, 3) \\ w_{x\tau\mu}^{(2)} \equiv \rho_{x+\hat{\mu}} \rho_x \text{Tr}(\tau_r V(x, \mu)) & (\mu = 1, 2, 3) \end{cases} \quad (13)$$

and in the H-channel:

$$h_x = \begin{cases} h_x^{(1)} \equiv \rho_x \\ h_x^{(2)} \equiv \text{Tr} V(x, \mu) \\ h_x^{(3)} \equiv \rho_{x+\hat{\mu}} \rho_x \text{Tr} V(x, \mu) \quad (\mu = 1, 2, 3, 4) \end{cases} \quad (14)$$

In the case of $\lambda = \infty$ the Higgs field length is frozen to $\rho_x = 1$, therefore in Eq. (13) only the first line and in Eq. (14) only the second one remain.

The W-mass could be determined with good precision in all the points, except for the 16^4 point at $(\lambda, \beta, \kappa) = (\infty, 8, 0.34)$. For an example of the time-slice correlations see Table VI (otherwise Ref. [7]). The W-correlations can be fitted very well with a single cosh (corresponding to a single state) for $d \geq 3$. The point $(\infty, 8, 0.34)$ is in this respect an exception, because the W-correlation for $d > 3$ is rather flat (see Fig. 2) and we could not find a stable cosh fit. The dominance of a single W-state is well demonstrated also by Figs. 3B - 3D, where the W-mass obtained from a single cosh between pairs of time-slices is shown. In contrast, on Fig. 3A for $(\infty, 8, 0.34)$ a clear decrease of the mass is observed for increasing time distances. On the 12^4 lattice the dominance of a single W-state is illustrated in the point $(0.1, 8, 0.177)$ by Fig. 4A. The summary of all W-mass values is contained in Table II.

The correlation in the H-channels is more difficult to determine, because the H-mass is much larger than the W-mass. Therefore, the value of the correlation at larger time separations is very small. Another, more subtle, problem is that for $R_{HW} \equiv m_H/m_W > 2$ the Higgs boson is not stable: it is a resonance in the multi-W channels. This later problem can only be considered at a later stage, when the large distance H-correlation will be calculated to a good precision. The reason is that the multi-W states couple only weakly to the local variables in Eq. (14), therefore their contribution is negligible for small distances (they will, however, dominate at some very large distances because of the smaller mass). In most cases we could determine the H-correlations with reasonable errors only for $d \leq 3$ (see, for instance, Table VI). In the points where am_H is less than 1 the situation is better, but still worse than for the W-channels: see Fig. 4B for the H-mass obtained from the time-slice pairs at $(\lambda = 0.1, \beta = 8, \kappa = 0.177)$. The best estimates we could obtain for the H-boson masses are given in Table II.

The summary of the masses in Table II shows that

- The W-masses on the 16^4 lattice are both at $(\lambda, \beta, \kappa) = (\infty, 8, 0.37)$ and $(\infty, 8, 0.42)$ about 10% smaller than on 12^4 .
- In the 12^4 points with approximately constant link expectation value L (see Table I) the W-mass is, within errors, independent of λ . For constant β and L the mass ratio R_{HW} is increasing with λ (see also Fig. 5). The upper limit of R_{HW} at $\beta = 8$ is about $\simeq 7$ on the 12^4 and about $\simeq 8$ on the 16^4 lattice. The mass ratio at $\lambda = \infty$ and $\beta = 8$ is not very sensitive to κ .

- The upper limit of R_{HW} at $\beta = 10$, which from the point of view of the renormalized SU(2) gauge coupling corresponds quite well to the phenomenological situation in the standard model, is about $R_{HW}^{max} \simeq 9$.

4 Conclusion

The aim of the present numerical calculation in the standard SU(2) Higgs model was to explore the qualitative behaviour of the dependence of physical variables on the bare parameters in a region of weak gauge coupling and strongest possible scalar self-coupling. The obtained upper limit for the Higgs boson mass $m_H \leq 9m_W$ is only a first crude estimate which can be improved considerably in future Monte Carlo studies. Since the renormalized gauge coupling turned out to be near to its physical value in our $\beta = 10$ point, future numerical calculations should be concentrated near $\beta = 10$. Of course, even a more precise value obtained in the Higgs sector is still approximate, because the coupling to fermions and the electromagnetic U(1) coupling are neglected.

Staying within the standard SU(2) Higgs model, there are three main sources of errors coming from the small lattice size and from the limited statistical accuracy:

- (a) Due to the limited statistics at $\beta = 10$ the Higgs mass was determined from the correlations at distances $d \leq 3$. This presumably implies that am_H is actually smaller than the value in Table II, because of the contributions of excited states at short distances.
- (b) The W-mass on a larger lattice is probably smaller. (This is the trend we saw by comparing 12^4 and 16^4 lattices in the same points.)
- (c) Since the H-mass in lattice units in our $\beta = 10$ point is about 1.8, the upper limit for R_{HW} at $\kappa = 0.42$ is almost certainly an overestimate, because the upper limit is most probably a monotonously decreasing function of the cut-off (and the cut-off is proportional to $(am_H)^{-1}$).

The points (a-b) have an opposite effect on the Higgs- to W-mass ratio and could together effect the upper limit only moderately. A much more important effect seems to be (c), which could easily reduce the upper limit by a factor of 2. Namely, in order to be able to talk about a quasi-continuum effective theory, one has to require something like $am_H \leq \frac{1}{2}$ (see the recent study of this question in the 1-component ϕ^4 model [11]). The upper limit for the mass ratio at $am_H = \frac{1}{2}$ can be substantially smaller than its value at $am_H \simeq 1.8$. For the numerical determination of a better upper limit one has to go, in the vicinity of $\beta = 10$, closer to the phase transition line, which means decreasing κ (and L). On the technical side $am_H \simeq \frac{1}{2}$ could require a lattice by a factor of 2 larger in linear size (i. e. 32^4).

In view of this, admittedly speculative, evaluation of possible systematic errors, the upper limit $R_{HW}^{max} \simeq 9$ is surprisingly low. The real upper limit for the Higgs boson mass belonging to a cut-off, say, 1 TeV could be easily as low as $\simeq 6m_W$. Note in this respect, that the use of the tree-level formula for the Higgs boson mass plus approximate block-spin transformation in the four-component ϕ^4 model seems to give somewhat higher upper limits [12]. Since the Higgs sector is the only unknown piece of the standard model, the improvement of the upper

limit for the Higgs mass certainly deserves further effort, especially as long as the Higgs boson is not yet found experimentally.

Acknowledgement

It is a pleasure to thank the staff of the Computer Centre of IABG, Ottobrunn and in particular Mr. E. Pahlberg, Mrs. H. Koste and Mr. U. Harms for their kind support of the computation on the Fujitsu VP-200.

References

- [1] R. Dashen, H. Neuberger, Phys. Rev. Lett. **50** (1983) 1897
- [2] W. Langguth, I. Montvay, P. Weisz, Nucl. Phys. **B277** (1986) 11
- [3] A. Hasenfratz, P. Hasenfratz, Tallahassee preprint FSU-SCRI-86-30, 1986
- [4] I. Montvay, Phys. Lett. **B172** (1986) 71
- [5] I. Montvay, DESY preprint 86-143 (1986), to appear in the Proceedings of the 1986 Brookhaven Conference on Lattice Gauge Theory, and DESY preprint 87-019 (1987)
- [6] I. Montvay, Nucl. Phys. **B269** (1986) 170
- [7] Tables of the Monte Carlo data can be obtained from the authors upon request.
- [8] M. Marcu, I. Montvay, in preparation.
- [9] W. J. Marciano, Phys. Rev. **D20** (1979) 274
- [10] UA1 Collaboration, Phys. Lett. **B126** (1983) 398
UA2 Collaboration, Phys. Lett. **B129** (1983) 130
- [11] M. Lüscher, P. Weisz, DESY preprint 87-017 (1987)
- [12] P. Hasenfratz, J. Nager, Bern preprint BUTP-86/20 (1986)

Table I

Summary of the points where the Monte Carlo calculations were performed. The average quantities in Eq. (6) are also given.

| λ | β | κ | <i>lattice</i> | <i>sweeps</i> | L | P | ρ |
|-----------|---------|----------|----------------|---------------|--------------|-------------|-------------|
| 0.1 | 8.0 | 0.177 | 12^4 | 113000 | 0.38164(12) | 0.09592(1) | 1.47464(11) |
| 0.1 | 8.0 | 0.182 | 12^4 | 98000 | 0.46227(7) | 0.09565(2) | 1.55315(7) |
| 1.0 | 8.0 | 0.28 | 12^4 | 200000 | 0.36947(6) | 0.09599(1) | 1.15598(2) |
| ∞ | 8.0 | 0.37 | 12^4 | 115000 | 0.36919(3) | 0.09600(1) | 1.0 |
| ∞ | 8.0 | 0.42 | 12^4 | 120000 | 0.46328(3) | 0.09579(3) | 1.0 |
| ∞ | 8.0 | 0.34 | 16^4 | 65000 | 0.28965(3) | 0.096198(3) | 1.0 |
| ∞ | 8.0 | 0.37 | 16^4 | 108000 | 0.36923(2) | 0.096013(3) | 1.0 |
| ∞ | 8.0 | 0.42 | 16^4 | 64000 | 0.463310(14) | 0.095743(3) | 1.0 |
| ∞ | 10.0 | 0.42 | 16^4 | 89000 | 0.469211(12) | 0.076238(2) | 1.0 |

Table II

Summary of the masses. The estimated errors in the last numerals are given in parenthesis. The last column is the H-mass to W-mass ratio.

| λ | β | κ | <i>lattice</i> | am_W | am_H | R_{HW} |
|-----------|---------|----------|----------------|----------|---------|---------------|
| 0.1 | 8.0 | 0.177 | 12^4 | 0.207(8) | 0.73(5) | 3.5 ± 0.4 |
| 0.1 | 8.0 | 0.182 | 12^4 | 0.243(9) | 0.98(7) | 4.0 ± 0.4 |
| 1.0 | 8.0 | 0.28 | 12^4 | 0.194(7) | 1.1(1) | 5.7 ± 0.7 |
| ∞ | 8.0 | 0.37 | 12^4 | 0.195(9) | 1.3(2) | 6.7 ± 1.3 |
| ∞ | 8.0 | 0.42 | 12^4 | 0.244(6) | 1.7(3) | 7.0 ± 1.4 |
| ∞ | 8.0 | 0.34 | 16^4 | 0.13(2) | 0.8(1) | 6.2 ± 1.7 |
| ∞ | 8.0 | 0.37 | 16^4 | 0.172(7) | 1.4(1) | 8.1 ± 0.9 |
| ∞ | 8.0 | 0.42 | 16^4 | 0.217(5) | 1.7(2) | 7.8 ± 1.1 |
| ∞ | 10.0 | 0.42 | 16^4 | 0.198(7) | 1.8(2) | 9.1 ± 1.3 |

Table IIIA

Expectation values of the Wilson-loops $W_{R,T} = W_{T,R}$ on 16^4 lattice at $(\lambda = \infty, \beta = 8.0, \kappa = 0.34)$. Entries below the main diagonal are the Creutz-ratios. Statistical errors in the last numerals are given in parentheses.

| | $T = 1, 2$ | $T = 2, 3$ | $T = 3, 4$ | $T = 4, 5$ | $T = 5, 6$ | $T = 6, 7$ | $T = 7, 8$ | $T = 8$ |
|---------|-------------|--------------|--------------|--------------|--------------|--------------|--------------|--------------|
| $R = 1$ | 0.903802(3) | 0.838542(6) | 0.781564(10) | 0.729164(13) | 0.680457(15) | 0.635063(18) | 0.592718(22) | 0.553211(24) |
| $R = 2$ | 0.031716(6) | 0.753707(11) | 0.686877(14) | 0.628028(18) | 0.574792(21) | 0.526267(25) | 0.481918(27) | 0.441357(29) |
| $R = 3$ | 0.022481(7) | 0.011535(9) | 0.618794(20) | 0.560938(24) | 0.509506(27) | 0.463163(31) | 0.421192(33) | 0.383123(36) |
| $R = 4$ | 0.020172(6) | 0.008592(9) | 0.005346(10) | 0.505781(29) | 0.457491(33) | 0.414352(37) | 0.375526(39) | 0.340486(42) |
| $R = 5$ | 0.019442(7) | 0.007592(9) | 0.004177(10) | 0.002921(10) | 0.412604(40) | 0.372822(44) | 0.337199(47) | 0.305188(50) |
| $R = 6$ | 0.019161(9) | 0.007163(14) | 0.003676(9) | 0.002349(10) | 0.001742(20) | 0.336288(49) | 0.303739(52) | 0.274597(55) |
| $R = 7$ | 0.019027(8) | 0.006955(15) | 0.003402(10) | 0.002037(13) | 0.001374(11) | 0.000954(29) | 0.274078(55) | 0.247614(58) |
| $R = 8$ | 0.018940(8) | 0.006814(10) | 0.003217(15) | 0.001795(17) | 0.001117(20) | 0.000679(21) | 0.000362(31) | 0.223624(61) |

Table IIIB

Expectation values of the Wilson-loops $W_{R,T} = W_{T,R}$ on 16^4 lattice at $(\lambda = \infty, \beta = 8.0, \kappa = 0.37)$. Entries below the main diagonal are the Creutz-ratios. Statistical errors in the last numerals are given in parentheses.

| | $T = 1, 2$ | $T = 2, 3$ | $T = 3, 4$ | $T = 4, 5$ | $T = 5, 6$ | $T = 6, 7$ | $T = 7, 8$ | $T = 8$ |
|---------|-------------|--------------|--------------|--------------|--------------|--------------|--------------|--------------|
| $R = 1$ | 0.903987(3) | 0.838915(6) | 0.782099(8) | 0.729836(11) | 0.681249(14) | 0.635953(18) | 0.593693(20) | 0.554252(23) |
| $R = 2$ | 0.031472(7) | 0.754406(11) | 0.687840(16) | 0.629207(19) | 0.576142(22) | 0.527739(26) | 0.483499(29) | 0.443004(31) |
| $R = 3$ | 0.022247(6) | 0.011318(10) | 0.620089(21) | 0.562503(26) | 0.511278(29) | 0.465068(33) | 0.423212(36) | 0.385208(38) |
| $R = 4$ | 0.019935(8) | 0.008370(7) | 0.005123(13) | 0.507658(30) | 0.459590(34) | 0.416591(38) | 0.377877(41) | 0.342902(43) |
| $R = 5$ | 0.019215(5) | 0.007378(6) | 0.003990(8) | 0.002756(12) | 0.414927(40) | 0.375282(44) | 0.339769(46) | 0.307805(48) |
| $R = 6$ | 0.018948(6) | 0.006977(8) | 0.003500(16) | 0.002197(10) | 0.001602(26) | 0.338881(50) | 0.306436(52) | 0.277327(53) |
| $R = 7$ | 0.018791(6) | 0.006758(12) | 0.003226(8) | 0.001873(8) | 0.001232(19) | 0.000861(29) | 0.276858(56) | 0.250413(58) |
| $R = 8$ | 0.018728(8) | 0.006619(14) | 0.003033(10) | 0.001679(16) | 0.001009(11) | 0.000581(19) | 0.000320(35) | 0.226422(61) |

Table IIIC

Expectation values of the Wilson-loops $W_{R,T} = W_{T,R}$ on 16^4 lattice at $(\lambda = \infty, \beta = 8.0, \kappa = 0.42)$. Entries below the main diagonal are the Creutz-ratios. Statistical errors in the last numerals are given in parentheses.

| | $T = 1, 2$ | $T = 2, 3$ | $T = 3, 4$ | $T = 4, 5$ | $T = 5, 6$ | $T = 6, 7$ | $T = 7, 8$ | $T = 8$ |
|---------|--------------|--------------|--------------|--------------|--------------|--------------|--------------|--------------|
| $R = 1$ | 0.904257(3) | 0.839442(5) | 0.782850(8) | 0.730783(10) | 0.682355(13) | 0.637195(17) | 0.595046(18) | 0.555699(21) |
| $R = 2$ | 0.031108(7) | 0.755405(10) | 0.689217(13) | 0.630886(17) | 0.578052(20) | 0.529840(22) | 0.485731(25) | 0.445344(28) |
| $R = 3$ | 0.021902(6) | 0.011003(7) | 0.621947(19) | 0.564726(23) | 0.513763(27) | 0.467762(29) | 0.426035(32) | 0.388127(34) |
| $R = 4$ | 0.019606(7) | 0.008084(6) | 0.004879(9) | 0.510274(28) | 0.462485(32) | 0.419702(35) | 0.381115(40) | 0.346216(41) |
| $R = 5$ | 0.018896(3) | 0.007116(6) | 0.003753(11) | 0.002548(15) | 0.418106(38) | 0.378666(41) | 0.343258(44) | 0.311351(46) |
| $R = 6$ | 0.018615(10) | 0.006714(7) | 0.003269(13) | 0.002010(14) | 0.001409(16) | 0.342463(48) | 0.310099(49) | 0.281037(50) |
| $R = 7$ | 0.018483(11) | 0.006518(6) | 0.003006(13) | 0.001728(13) | 0.001101(10) | 0.000753(20) | 0.280582(52) | 0.254156(53) |
| $R = 8$ | 0.018396(7) | 0.006381(8) | 0.002850(13) | 0.001524(15) | 0.000844(14) | 0.000510(16) | 0.000260(35) | 0.230160(55) |

Table IIID

Expectation values of the Wilson-loops $W_{R,T} = W_{T,R}$ on 16^4 lattice at $(\lambda = \infty, \beta = 10.0, \kappa = 0.42)$. Entries below the main diagonal are the Creutz-ratios. Statistical errors in the last numerals are given in parentheses.

| | $T = 1, 2$ | $T = 2, 3$ | $T = 3, 4$ | $T = 4, 5$ | $T = 5, 6$ | $T = 6, 7$ | $T = 7, 8$ | $T = 8$ |
|---------|-------------|-------------|--------------|--------------|--------------|--------------|--------------|--------------|
| $R = 1$ | 0.923762(2) | 0.871411(3) | 0.824989(5) | 0.781627(7) | 0.740694(10) | 0.701955(12) | 0.665263(15) | 0.630501(18) |
| $R = 2$ | 0.024138(4) | 0.802423(7) | 0.746878(10) | 0.696930(12) | 0.650806(15) | 0.607907(19) | 0.567911(22) | 0.530591(24) |
| $R = 3$ | 0.016990(4) | 0.008547(4) | 0.689261(14) | 0.639129(17) | 0.593531(20) | 0.551513(23) | 0.512613(26) | 0.476546(28) |
| $R = 4$ | 0.015225(4) | 0.006297(4) | 0.003821(8) | 0.590383(21) | 0.546644(25) | 0.506640(28) | 0.469788(31) | 0.435755(33) |
| $R = 5$ | 0.014683(6) | 0.005544(3) | 0.002956(5) | 0.002010(7) | 0.505130(29) | 0.467425(33) | 0.432841(36) | 0.401004(39) |
| $R = 6$ | 0.014472(7) | 0.005236(4) | 0.002573(6) | 0.001580(5) | 0.001137(11) | 0.432042(38) | 0.399722(42) | 0.370058(45) |
| $R = 7$ | 0.014370(5) | 0.005086(5) | 0.002376(5) | 0.001350(6) | 0.000884(10) | 0.000603(12) | 0.369598(46) | 0.342026(49) |
| $R = 8$ | 0.014307(7) | 0.004983(6) | 0.002244(8) | 0.001196(10) | 0.000712(12) | 0.000418(14) | 0.000202(20) | 0.316447(55) |

Table IV

Expectation values of the Wilson-loops $W_{R,T} = W_{T,R}$ on 12^4 lattice at $(\lambda = \infty, \beta = 8.0, \kappa = 0.37)$. Entries below the main diagonal are the Creutz-ratios. Statistical errors in the last numerals are given in parentheses. The errors of the Creutz-ratios are calculated from the errors of the largest Wilson-loop only.

| | $T = 1, 2$ | $T = 2, 3$ | $T = 3, 4$ | $T = 4, 5$ | $T = 5, 6$ | $T = 6$ |
|---------|-------------|-------------|-------------|-------------|-------------|-------------|
| $R = 1$ | 0.90400(1) | 0.83892(1) | 0.78209(2) | 0.72982(3) | 0.68121(4) | 0.63591(5) |
| $R = 2$ | 0.03146(4) | 0.75443(3) | 0.68786(4) | 0.62924(5) | 0.57618(7) | 0.52783(8) |
| $R = 3$ | 0.02222(6) | 0.01123(10) | 0.62017(6) | 0.56264(8) | 0.51148(9) | 0.46542(11) |
| $R = 4$ | 0.01990(8) | 0.00827(14) | 0.00498(20) | 0.50792(10) | 0.46001(12) | 0.41729(13) |
| $R = 5$ | 0.01917(12) | 0.00724(18) | 0.00373(26) | 0.00241(34) | 0.41562(14) | 0.37638(15) |
| $R = 6$ | 0.01882(15) | 0.00674(24) | 0.00311(31) | 0.00170(40) | 0.00090(50) | 0.34053(17) |

Table V

The correlation of the Wilson-loops on the 16^4 lattice at $(\lambda = \infty, \beta = 10.0, \kappa = 0.42)$. Above the main diagonal the first length is fixed to 1, below the main diagonal to 8. Statistical errors were obtained by binning the data sequence.

| | $T_2 = 1$ | $T_2 = 2$ | $T_2 = 3$ | $T_2 = 4$ | $T_2 = 5$ | $T_2 = 6$ | $T_2 = 7$ | $T_2 = 8$ |
|--------------|------------|-------------|-------------|-------------|-------------|-------------|-------------|-------------|
| $R_2 = 1$ | 1.90(5)E-8 | 3.12(8)E-8 | 4.10(11)E-8 | 4.95(13)E-8 | 5.72(18)E-8 | 6.38(20)E-8 | 6.94(25)E-8 | 7.44(28)E-8 |
| $R_2 = 1, 2$ | 1.19(3)E-6 | 6.36(15)E-8 | 8.93(23)E-8 | 1.12(3)E-7 | 1.32(4)E-7 | 1.50(4)E-7 | 1.65(5)E-7 | 1.79(5)E-7 |
| $R_2 = 2, 3$ | 1.35(3)E-6 | 2.27(5)E-6 | 1.40(3)E-7 | 1.84(4)E-7 | 2.23(5)E-7 | 2.58(6)E-7 | 2.89(7)E-7 | 3.17(8)E-7 |
| $R_2 = 3, 4$ | 1.40(4)E-6 | 2.45(6)E-6 | 3.23(8)E-6 | 2.58(6)E-7 | 3.24(7)E-7 | 3.82(9)E-7 | 4.33(10)E-7 | 4.79(11)E-7 |
| $R_2 = 4, 5$ | 1.45(4)E-6 | 2.60(7)E-6 | 3.45(8)E-6 | 4.22(9)E-6 | 4.23(10)E-7 | 5.11(11)E-7 | 5.88(13)E-7 | 6.57(14)E-7 |
| $R_2 = 5, 6$ | 1.51(5)E-6 | 2.73(7)E-6 | 3.66(9)E-6 | 4.49(10)E-6 | 5.21(12)E-6 | 6.35(13)E-7 | 7.43(15)E-7 | 8.40(18)E-7 |
| $R_2 = 6, 7$ | 1.58(5)E-6 | 2.89(8)E-6 | 3.87(10)E-6 | 4.76(11)E-6 | 5.53(12)E-6 | 6.26(14)E-6 | 8.89(18)E-7 | 1.02(2)E-6 |
| $R_2 = 7, 8$ | 1.64(5)E-6 | 3.00(8)E-6 | 4.05(10)E-6 | 5.00(12)E-6 | 5.82(13)E-6 | 6.59(15)E-6 | 7.30(16)E-6 | 1.19(2)E-6 |
| $R_2 = 8$ | 1.69(6)E-6 | 3.09(9)E-6 | 4.18(11)E-6 | 5.18(12)E-6 | 6.05(14)E-6 | 6.87(15)E-6 | 7.64(17)E-6 | 8.34(18)E-6 |

Table VI

The zero momentum correlations as a function of the time-slice distance T on the 16^4 lattice at $(\lambda = \infty, \beta = 8.0, \kappa = 0.37)$.

| | $T = 0$ | $T = 1$ | $T = 2$ | $T = 3$ | $T = 4$ | $T = 5$ | $T = 6$ | $T = 7$ | $T = 8$ |
|-----------|----------------------------------|----------------------------------|----------------------------------|----------------------------------|----------------------------------|----------------------------------|----------------------------------|----------------------------------|----------------------------------|
| H-channel | 7.35E-05 $\pm 8.0\text{E-}08$ | 9.23E-06 $\pm 6.5\text{E-}08$ | 2.09E-06 $\pm 6.0\text{E-}08$ | 5.09E-07 $\pm 5.7\text{E-}08$ | 1.67E-07 $\pm 6.1\text{E-}08$ | 1.67E-07 $\pm 5.7\text{E-}08$ | 2.40E-08 $\pm 5.5\text{E-}08$ | 3.13E-08 $\pm 6.2\text{E-}08$ | 9.20E-08 $\pm 8.2\text{E-}08$ |
| W-channel | 4.78E-05 $\pm 1.1\text{E-}07$ | 8.36E-06 $\pm 1.1\text{E-}07$ | 5.86E-06 $\pm 1.1\text{E-}07$ | 4.98E-06 $\pm 1.0\text{E-}07$ | 4.44E-06 $\pm 1.0\text{E-}07$ | 4.04E-06 $\pm 1.0\text{E-}07$ | 3.77E-06 $\pm 1.0\text{E-}07$ | 3.60E-06 $\pm 1.1\text{E-}07$ | 3.58E-06 $\pm 1.1\text{E-}07$ |

Figure captions

Fig. 1A. The Yukawa potential obtained at $(\lambda = \infty, \beta = 8, \kappa = 0.34)$ on a 16^4 lattice. The circles show the values given by Eq. (9). The line connects the extrapolated $T = \infty$ values obtained by the two-exponential fits. The statistical errors are in most cases smaller than the circles.

Fig. 1B. The same as Fig. 1A, for $(\lambda = \infty, \beta = 8, \kappa = 0.37)$.

Fig. 1C. The same as Fig. 1A, for $(\lambda = \infty, \beta = 8, \kappa = 0.42)$.

Fig. 1D. The same as Fig. 1A, for $(\lambda = \infty, \beta = 10, \kappa = 0.42)$.

Fig. 2. The W -correlation as a function of the time-slice distance on 16^4 lattice at $(\lambda = \infty, \beta = 8, \kappa = 0.34)$.

Fig. 3A. The W -mass determined from a single cosh between time-slice pairs on 16^4 lattice at $(\lambda = \infty, \beta = 8, \kappa = 0.34)$. Identical symbols belong to the same time-slice distance. The dotted horizontal line is the mass given in Table II.

Fig. 3B. The same as Fig. 3A, for $(\lambda = \infty, \beta = 8, \kappa = 0.37)$.

Fig. 3C. The same as Fig. 3A, for $(\lambda = \infty, \beta = 8, \kappa = 0.42)$.

Fig. 3D. The same as Fig. 3A, for $(\lambda = \infty, \beta = 10, \kappa = 0.42)$.

Fig. 4A. The same as Fig. 3A for the W -mass on 12^4 lattice at $(\lambda = 0.1, \beta = 8, \kappa = 0.177)$.

Fig. 4B. The same as Fig. 3A for the Higgs mass on 12^4 lattice at $(\lambda = 0.1, \beta = 8, \kappa = 0.177)$.

Fig. 5. The ratio of the Higgs mass to W -mass for $\beta = 8$ and nearly constant link expectation value (L) on 12^4 lattice as a function of λ^{-1} .

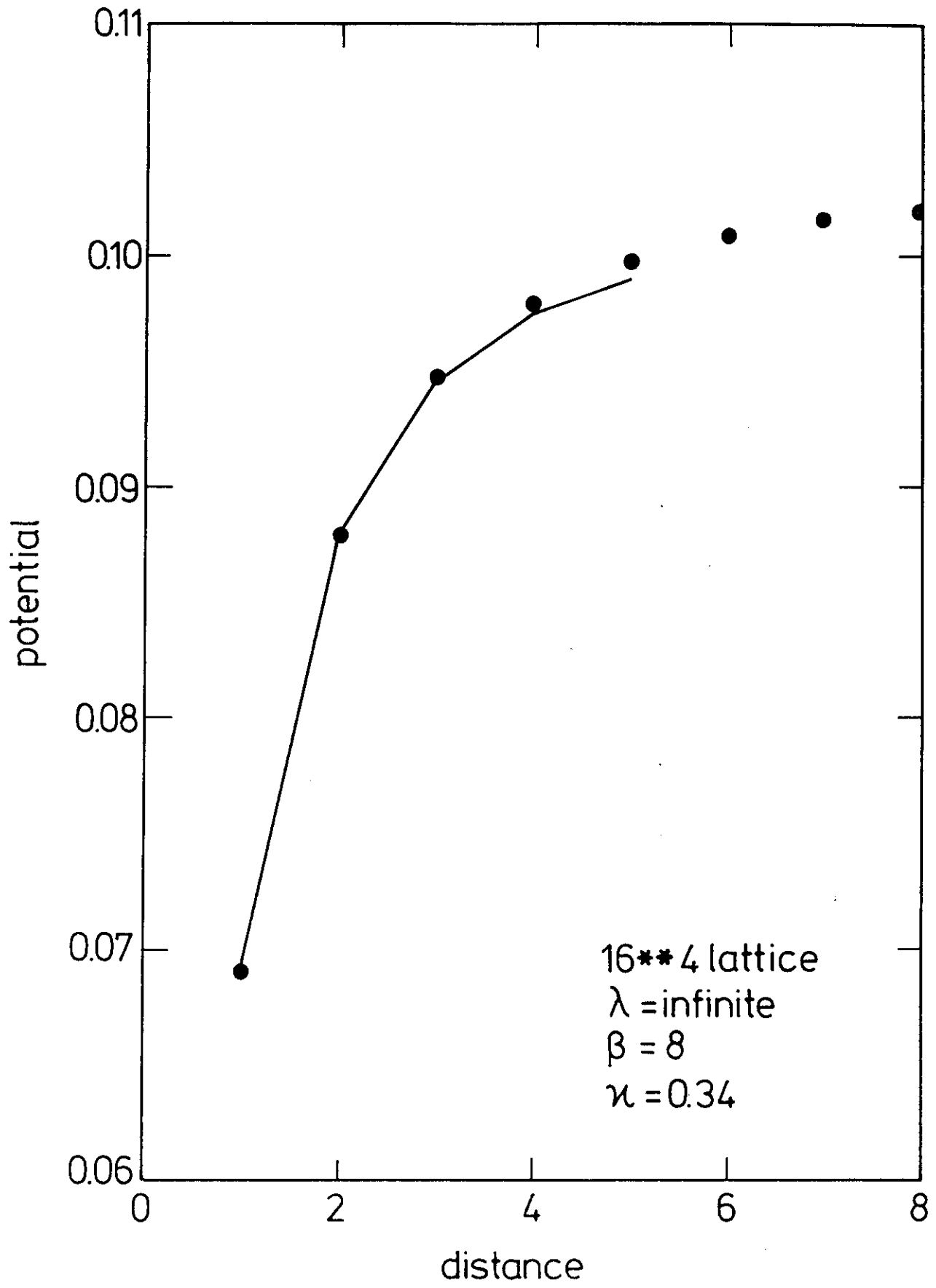


Fig. 1A

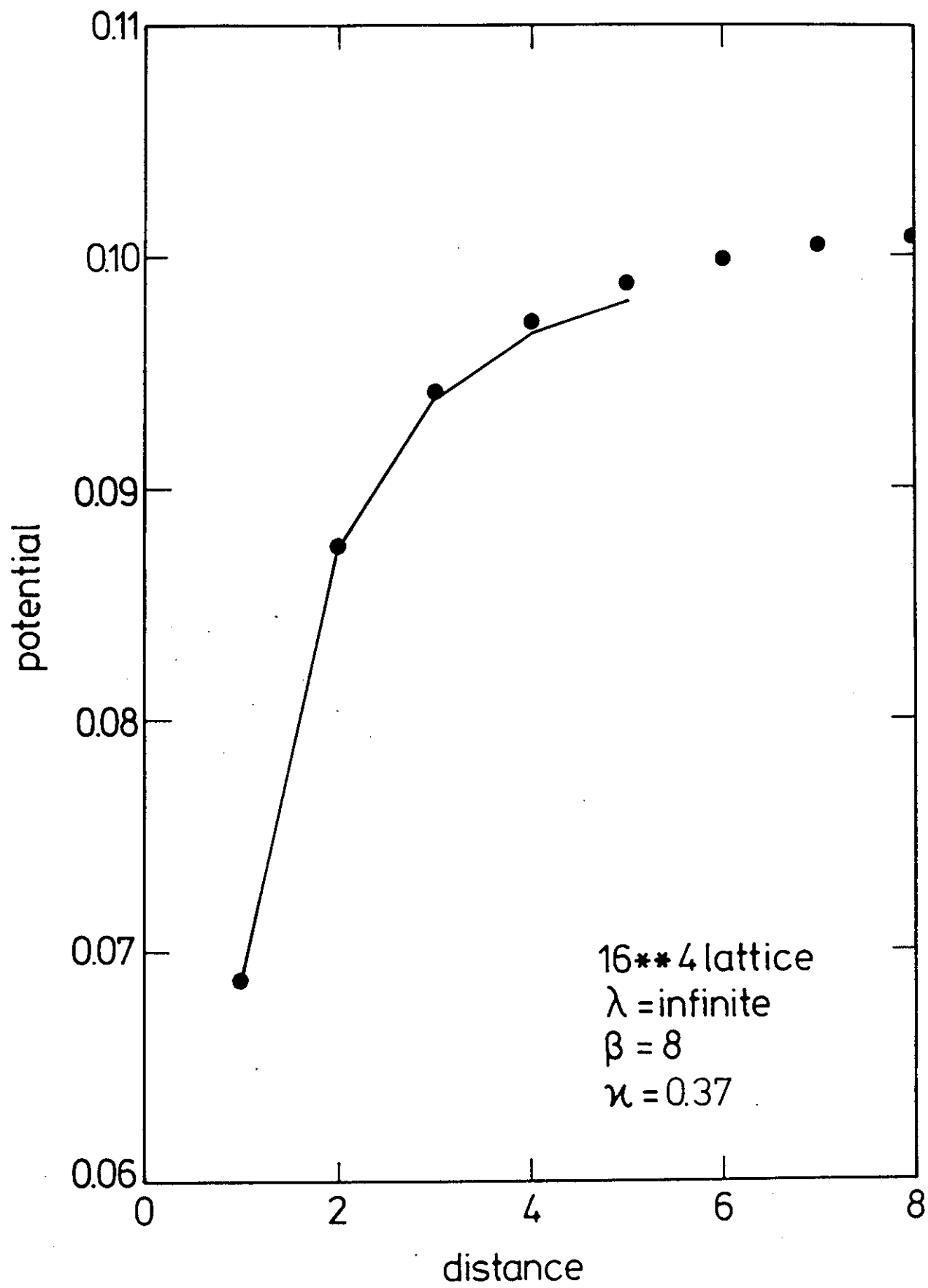


Fig.1B

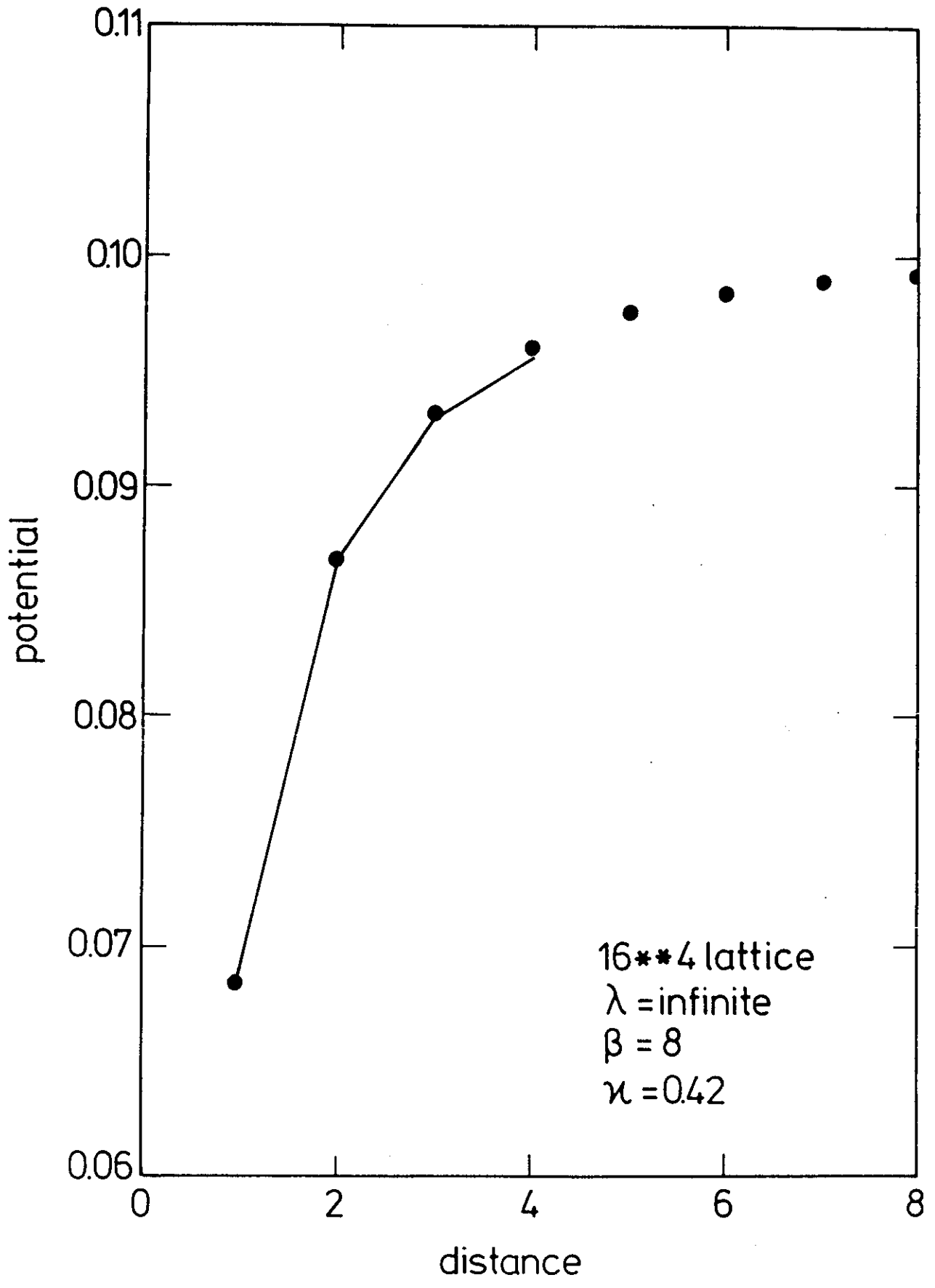


Fig.1C

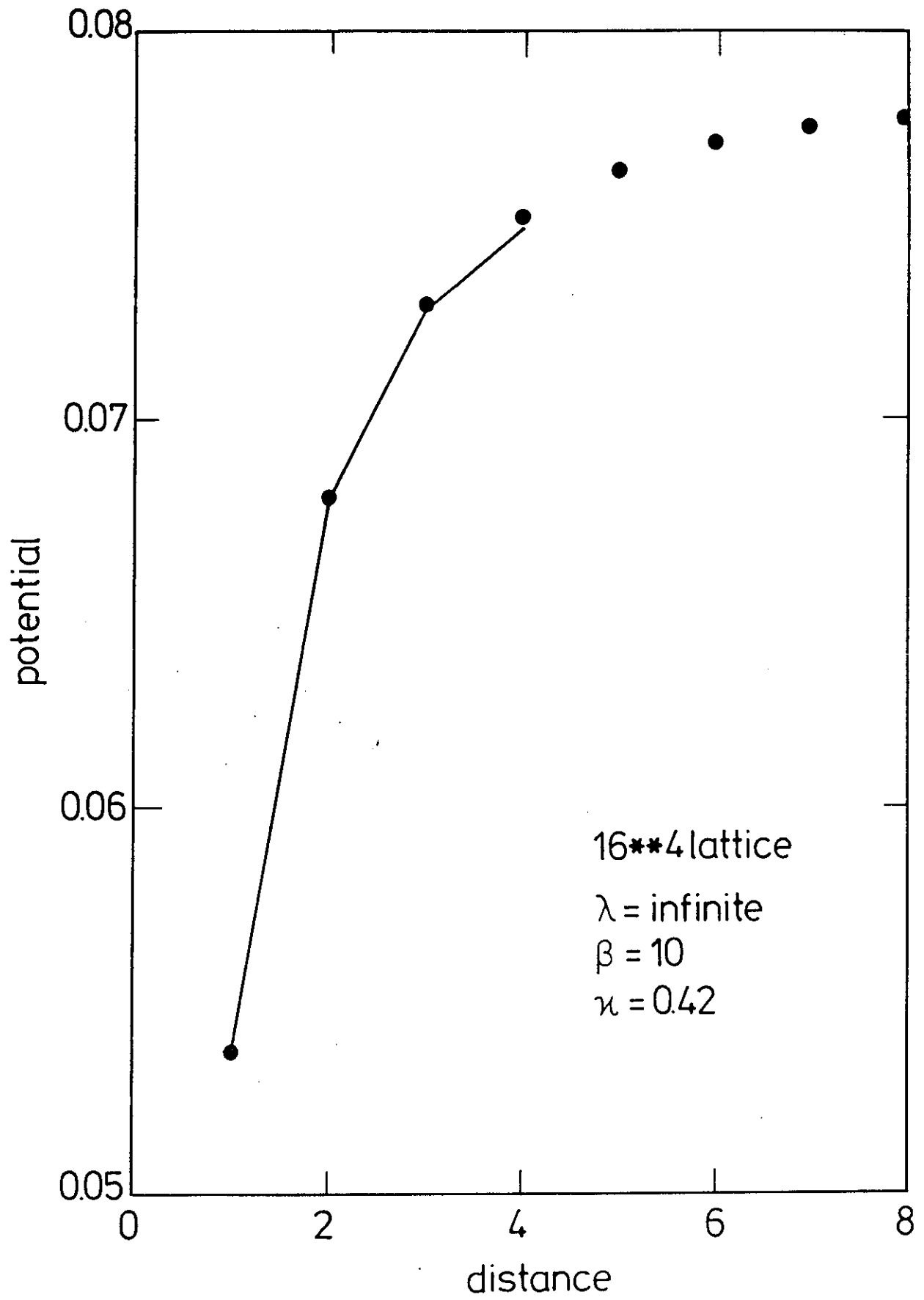


Fig. 1D

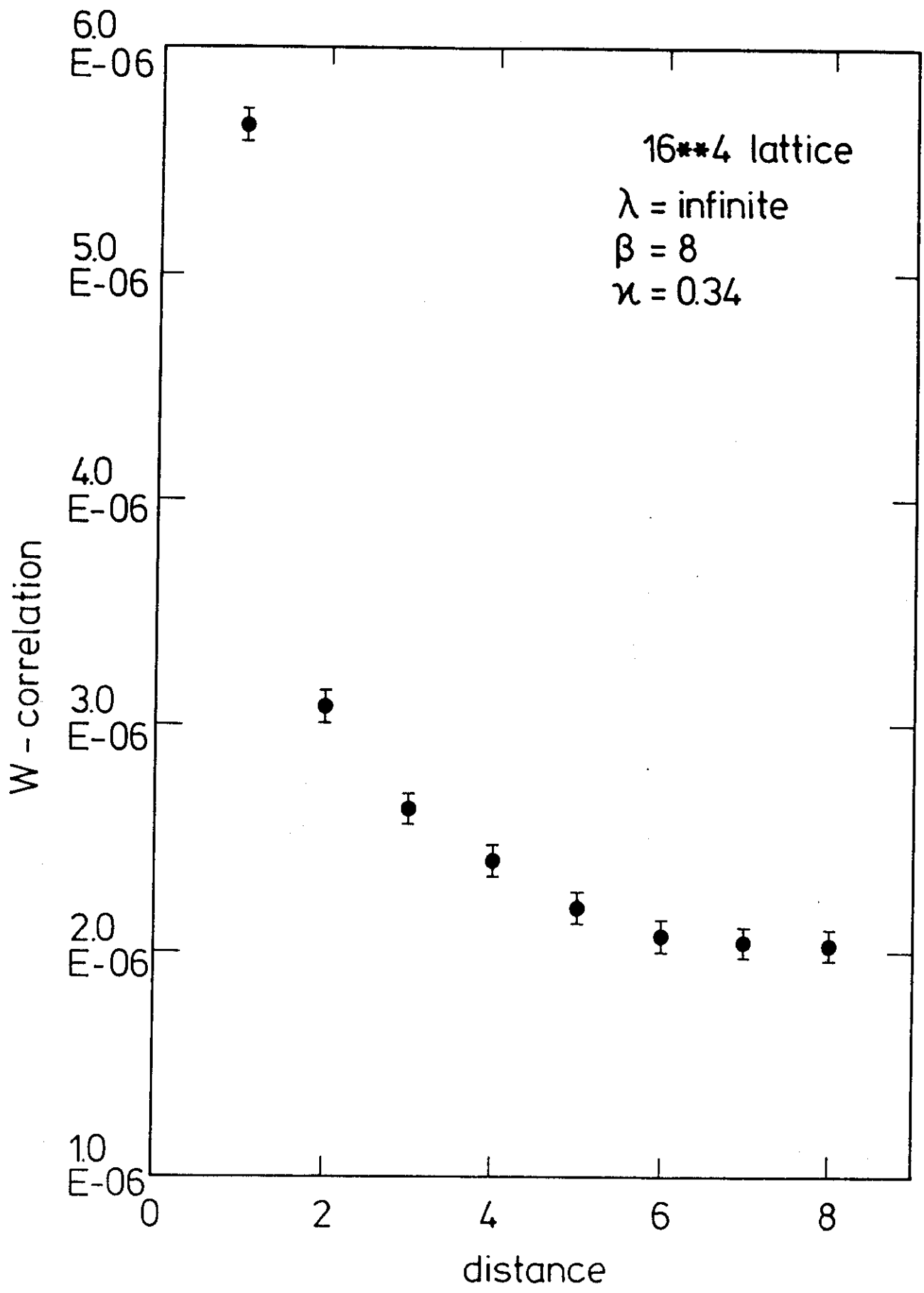
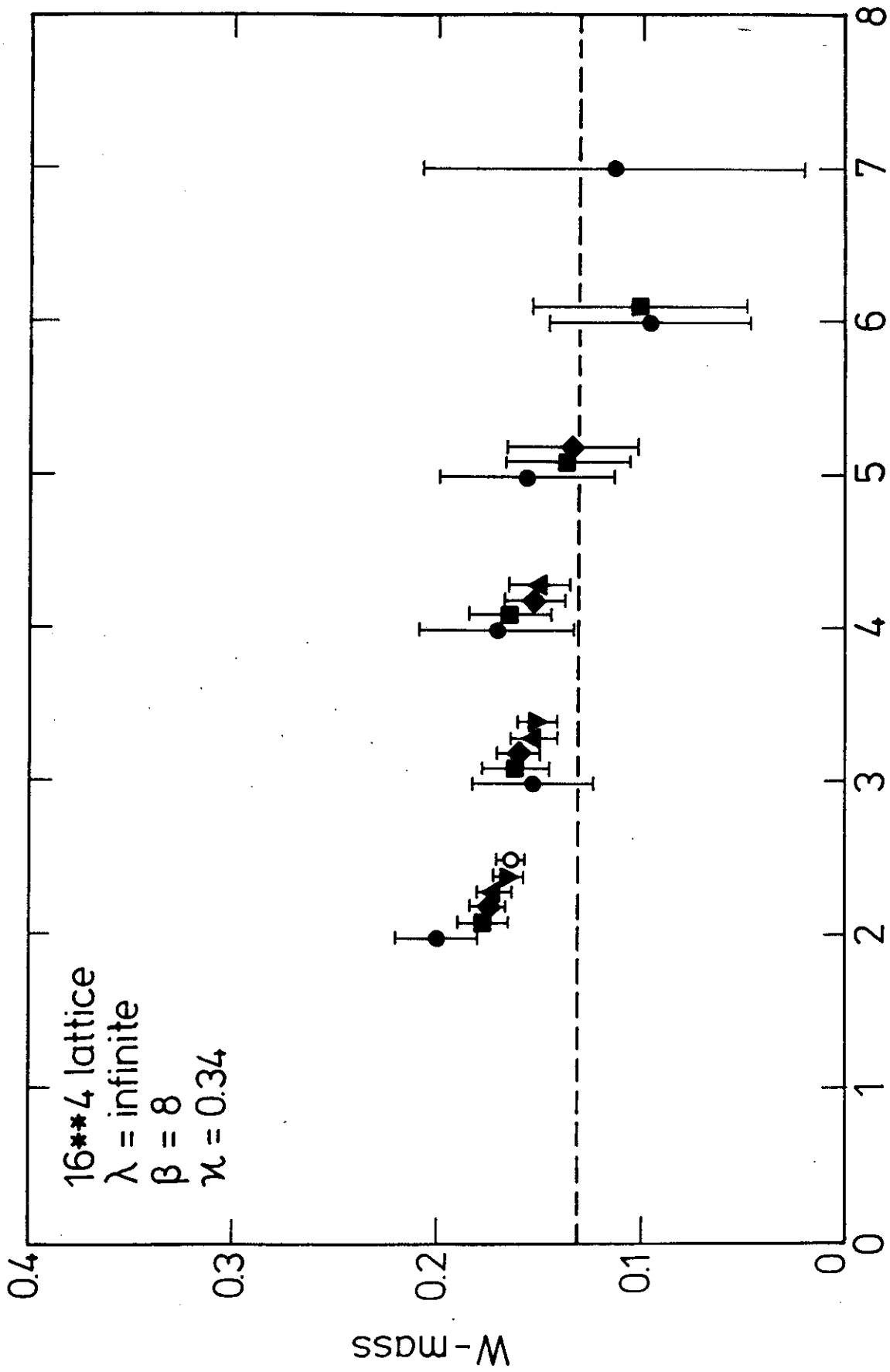
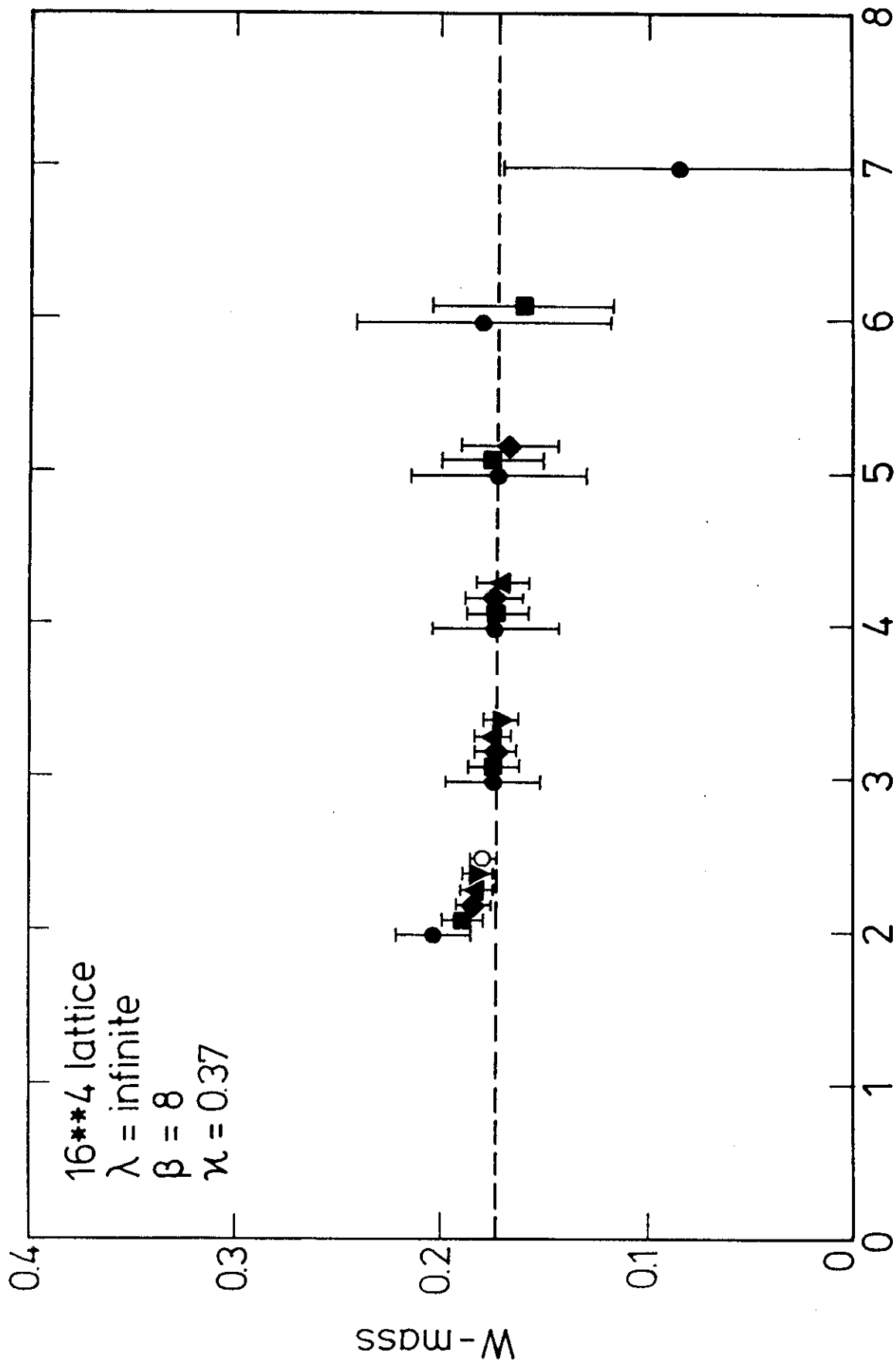


Fig.2



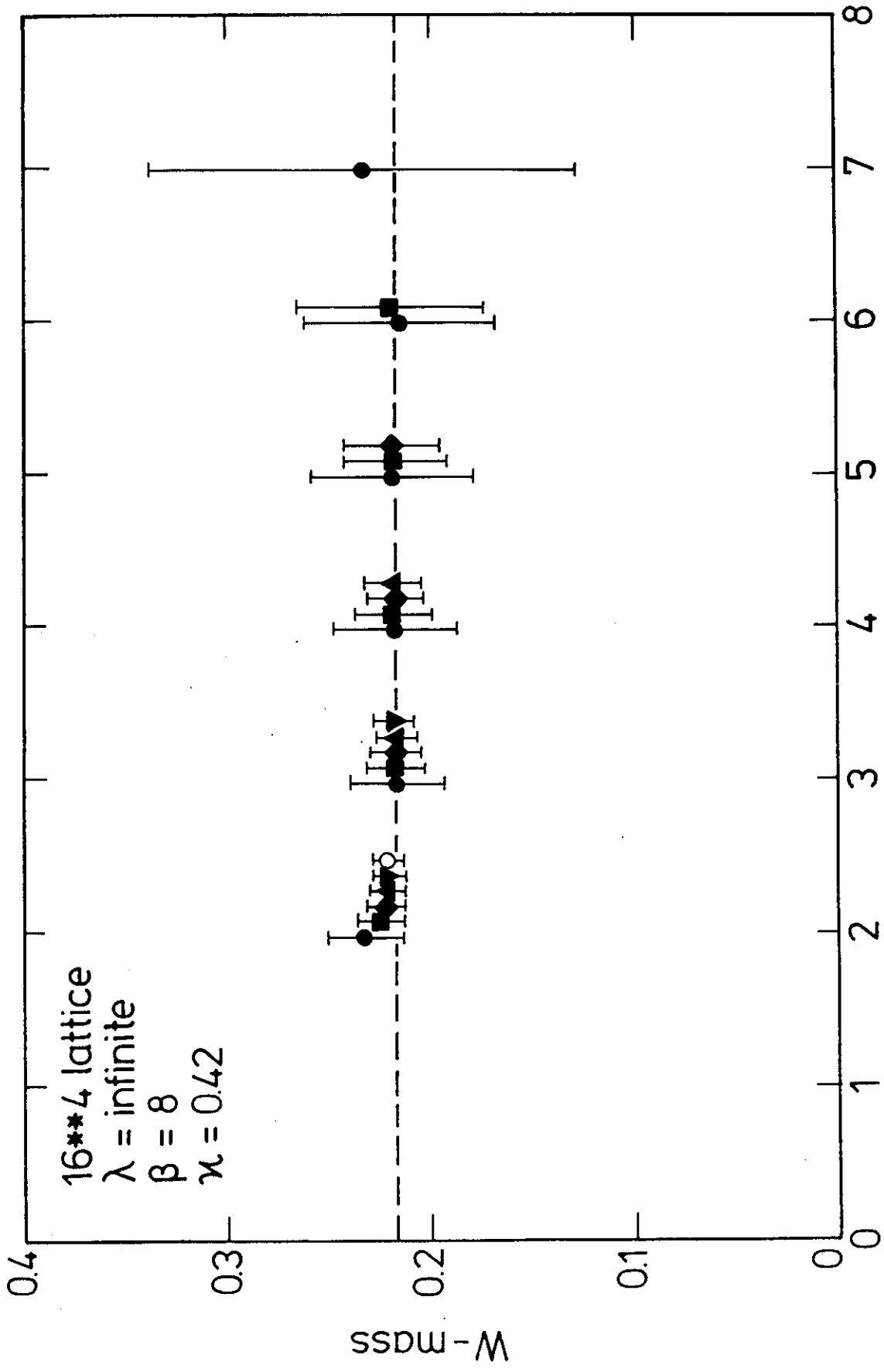
first timeslice

Fig. 3A

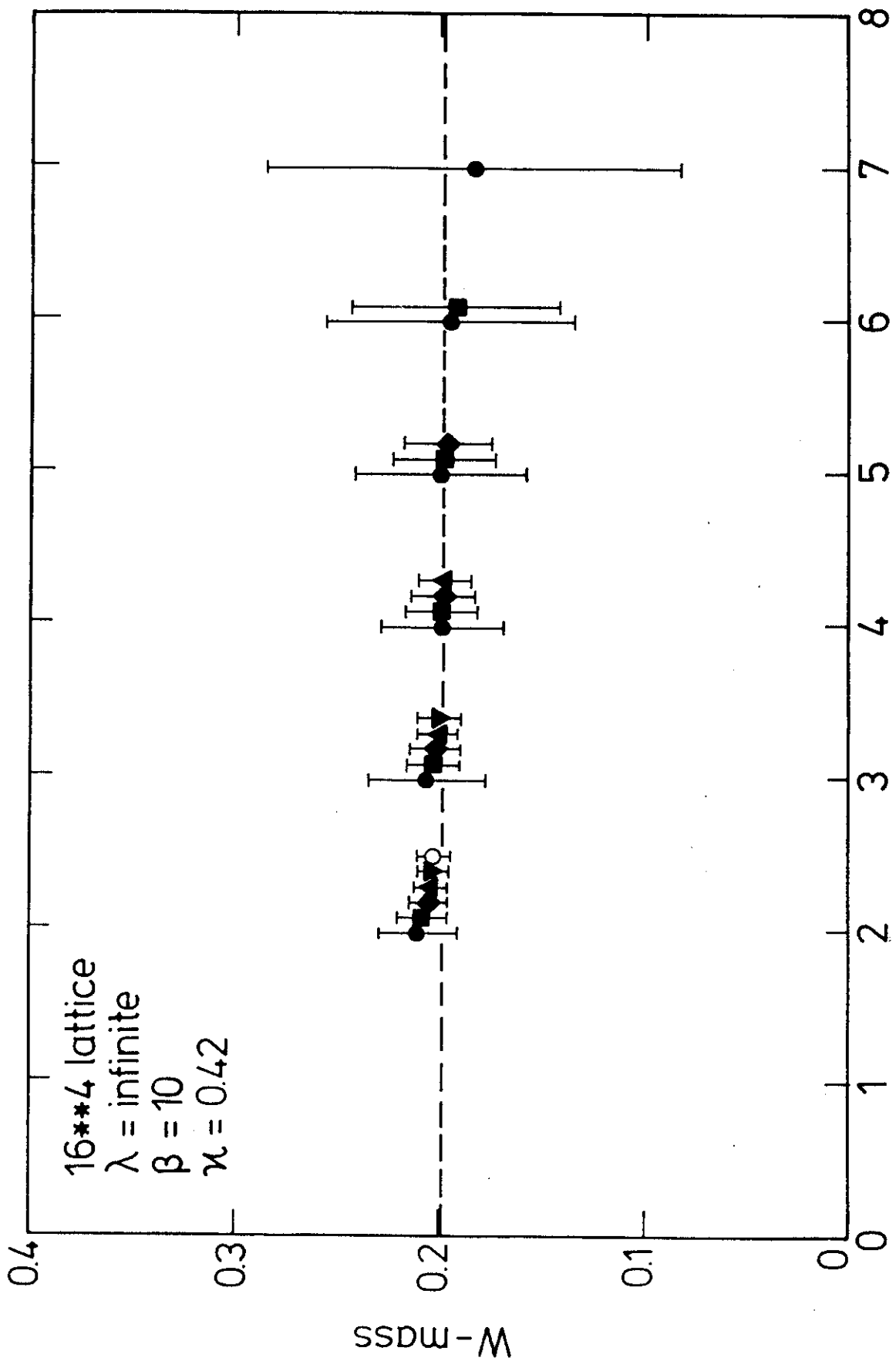


first timeslice

Fig.3B



first timeslice
Fig.3C



first timeslice

Fig.3D

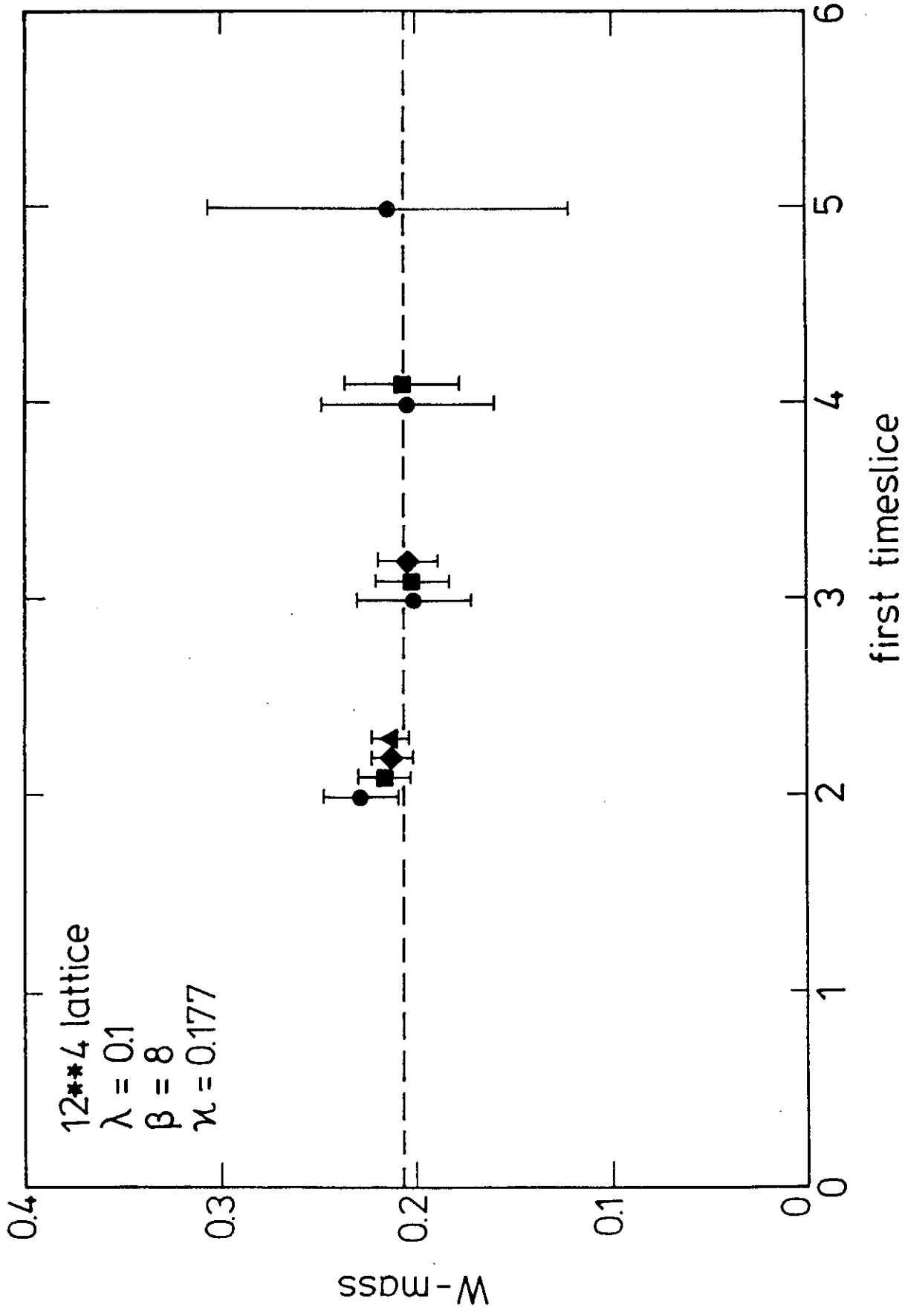


Fig.4A

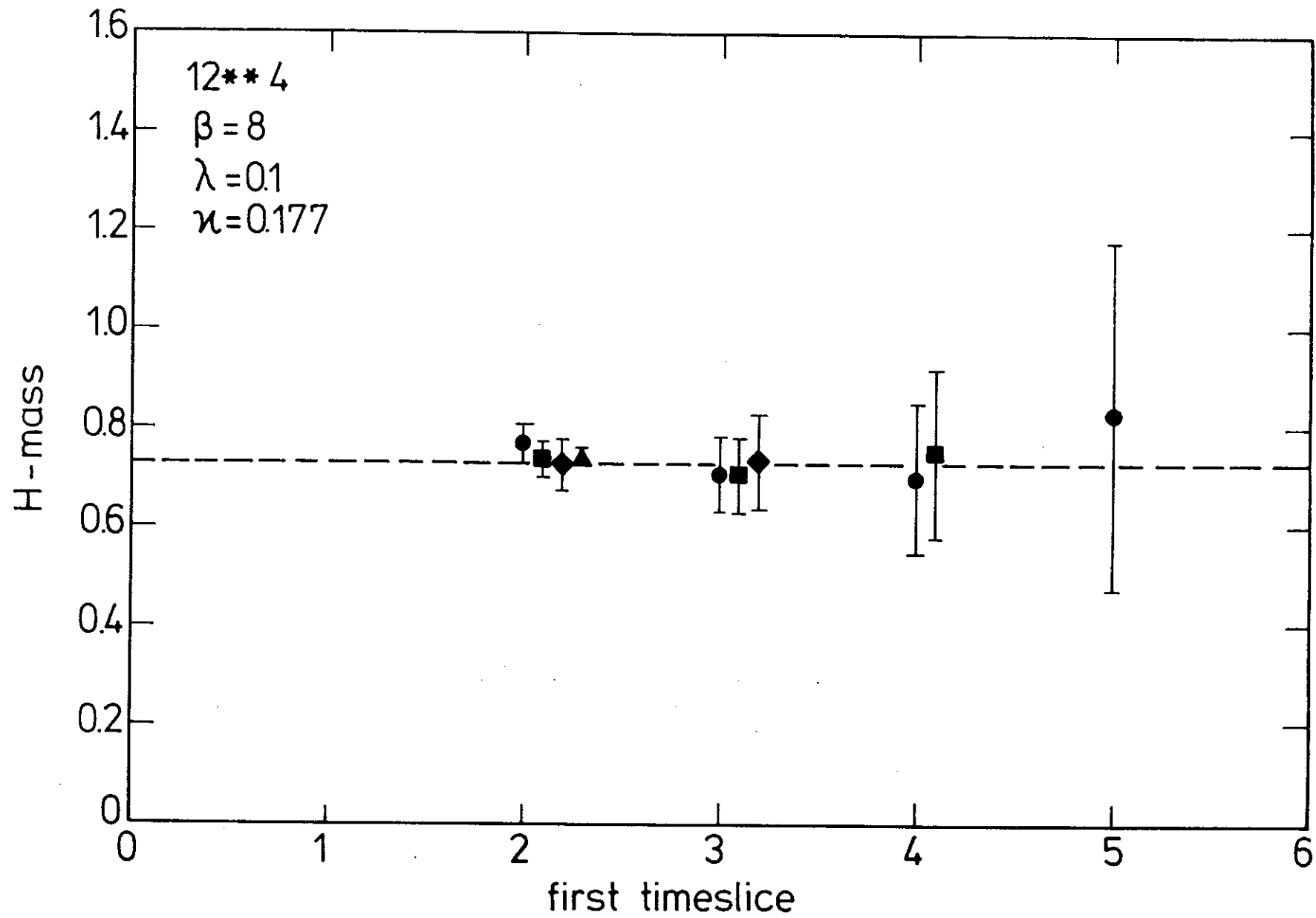


Fig.4B

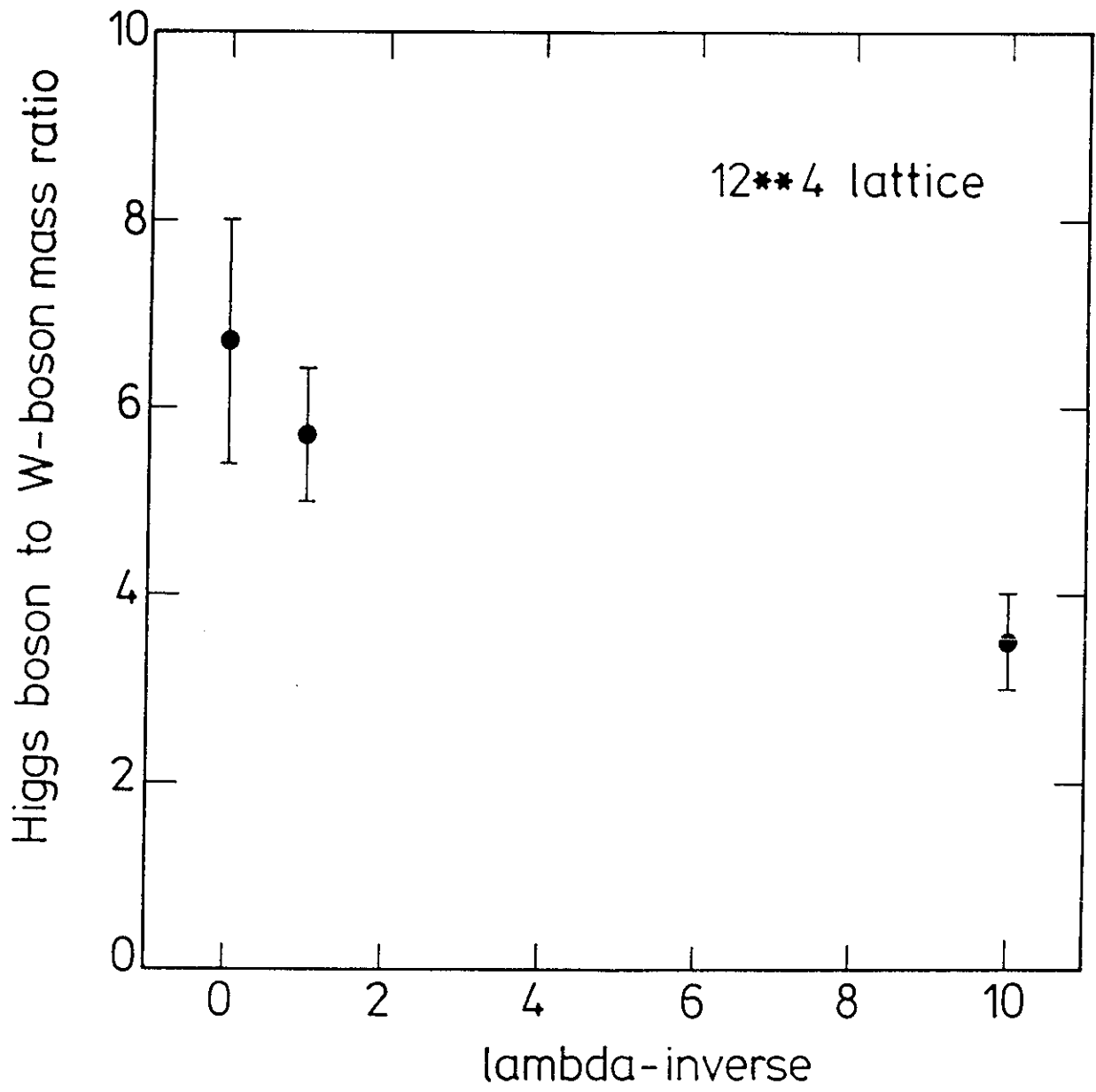


Fig.5